

Structural analysis of stone masonry columns of the Basilica S. Maria di Collemaggio

Pietro Crespi^{*}, Alberto Franchi, Nicola Giordano, Manuela Scamardo, Paola Ronca

Department of Architecture, Built Environment and Construction Engineering, Politecnico di Milano, Piazza Leonardo da Vinci 32, 20133 Milano, Italy

The Basilica of Collemaggio in L'Aquila is one of the outstanding architectural heritage in Abruzzo Region. The church, built in the late XIII century, has experienced many earthquakes during its life, some of which caused damages to the masonry structures, requiring continuous interventions and renovations. The last strong earthquake (April 6th, 2009) caused the collapse of the transept structures and significant damages in the apses area.

Since 2009, several research groups have focused their attention on the Basilica, both from architectural and structural point of view. Particularly, recent studies have pointed out the historical value of nave columns, which seem to be XIII century authentic elements.

Despite the magnitude of the last earthquake, the columns have proved limited resistance against seismic loads, resulting in a widespread damage, but without reaching the collapse. The aim of the present paper is to understand their structural behavior under horizontal actions.

An overall finite element model of the church has been developed to perform eigenvalue and response spectrum analyses of the Basilica.

Afterwards, a representative nave column has been studied considering both geometrical and mechanical non-linearity. In order to obtain a reliable evaluation of its structural behavior, two different models have been developed: an analytical model and a solid-brick finite element one.

The performed analyses have allowed the evaluation of the stresses redistribution inside the columns after cracking. The results, provided in terms of force-displacement curve and stress contours, have permitted to identify some possible explanations about the columns seismic response.

Keywords: Collemaggio, Historical church, Earthquake, Stone masonry columns, Finite element, Non-linear analysis

1. Introduction

Seismic assessment, preservation and retrofit of existing buildings are relevant topics today, especially in countries like Italy, where an important monumental heritage is built in moderate or high seismic zones.

Historic masonry structures, very different by type and construction techniques, represent the most part of this heritage. The structural analyses executed on these buildings are a challenging issue for engineers and researchers [1] because masonry structures are characterized by highly non-linear response under seismic loads (e.g. extensive cracks under tension and shear, crushing in compression, development of local collapse mechanisms, etc.). Furthermore, the knowledge of material and geometrical

parameters needed in the analysis is a key question when dealing with seismic assessment of existing masonry buildings. In most cases, the detailed geometrical survey of the building is not available and the inner composition of masonry is unknown. Moreover, the characterization of the material mechanical properties is difficult and often requires expensive in-situ tests (flat jacks [2], diagonal compression [3], etc.). Finally, especially for old buildings, the variability of these mechanical properties is strongly influenced by the construction history and the repairing interventions of the structure [4].

The Basilica S. Maria di Collemaggio is a well-known historical monument in Italy and for this reason was deeply studied in recent decades. In 2001, Antonacci et al. [5] investigated the dynamic behavior of the church performing hammer and vibrodine tests. The data collected from accelerometers monitoring system revealed some deficiencies in roof-to-wall connections, despite the low intensity of excitations. In 2004, Ranalli et al. [6] presented some experimental results conducted on the façade of the Basilica, using the ground penetrating radar technique. Their principal aim

Article history:

Available online 13 June 2016

^{*} Corresponding author.

E-mail addresses: pietro.crespi@polimi.it (P. Crespi), alberto.franchi@polimi.it (A. Franchi), nicola.giordano@polimi.it (N. Giordano), manuela.scamardo@polimi.it (M. Scamardo), paola.ronca@polimi.it (P. Ronca).

was the determination of wall thicknesses and the identification of possible damages of the façade, for restoration purposes. After the 2009 L'Aquila earthquake, significant contributions were given by Cimellaro et al. [7–9], Cartapati [10] and Ciampi [11] concerning the seismic response of the Basilica.

In 2013, Gattulli et al. [12] focused on the behavior of the Basilica during the April 6th, 2009 earthquake. They pointed out, with linear and non-linear analyses, the strong vulnerability of the transept structural system with respect to both transversal and longitudinal seismic actions. More recently, in 2015, new contributions were given on the comprehension of the church dynamic response (Potenza et al. [13]) and its structural failures (Arcidiacono et al. [14]).

The aim of the present paper is to understand the structural behavior of the naves stone masonry columns under horizontal actions. These elements, probably authentic from medieval age, overcame the last strong earthquake in spite of the severe damages they have experienced.

Firstly, the overall dynamic behavior of the church is checked out through eigenvalue and response spectrum analyses. Then, two different non-linear analyses of a representative stone masonry column are presented and discussed.

2. Description of the basilica

Built by the will of pope Celestine V in the late XIII century and placed on the top of a hill in the city of L'Aquila, the Basilica of Collemaggio is an outstanding example of Romanesque architecture in Abruzzo. During the centuries, the church construction process was characterized by several interventions, spread over the whole building, many of which were the result of earthquake damages [15].

The church has a three naves structure built on a basilical plan, separated by two lines of seven octagonal columns supporting pointed arches (Fig. 1a). A not-protruding-outside transept together with two chapels and a choir are placed at the opposite side of the façade. At the intersection of the central nave and transept, a low dome covered by a roof has been completely rebuilt during the XX century. The two altars at the far ends of the transept, together with the stucco decoration of walls, vaults and chapels are a residual of the baroque decoration removed in the seventies. The rest of the church shows bare walls with exposed wooden trusses to support a gable roof on the central nave and a pitched roof on the aisles.

Just at the right of the majestic two-tone façade (Fig. 1b), an unusual octagonal base squat tower is placed.

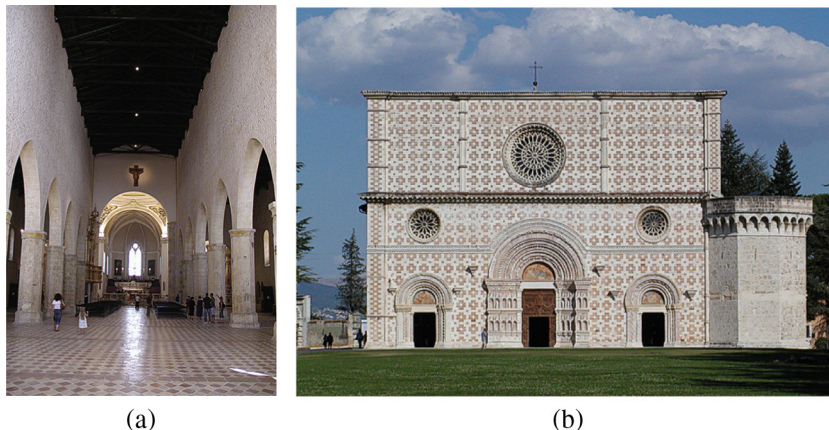


Fig. 1. (a) Central nave and octagonal columns; (b) Façade and octagonal base squat tower.

2.1. The evolution until the XIX century

Starting from the initial structure of XIII century, the construction activity continued until the XVI century. Probably because of the earthquakes of 1639 and 1654, in the XVII century the church underwent substantial changes, not only as an enrichment of the decorations in Baroque style, but also in order to improve the seismic resistance of the structures [14]. Among the interventions, the most relevant ones were the aisle walls lowering and the improved roof connection, both between vaults and walls, in the lateral naves (Fig. 2a), and between wooden ceiling and walls, in the central one (Fig. 2b).

2.2. The XX century reconstruction

The 1915 Fucino earthquake caused serious damages to the Basilica, particularly at the upper left corner of the façade (Fig. 3). The right part was left unharmed due to the presence of the tower and a buttress, probably built because of previous earthquake damages. The strengthening interventions consisted in realizing a new buttress in the left corner of the façade with strong tie rods to restrain any forward movement. To improve the out-of-plane stiffness, a reinforced concrete (r.c.) frame was built to reconstruct the façade wall [12]. In the reconstruction, lighter materials were used going to the top (stones, solid brick, hollow brick) to bring the center of gravity as low as possible.

Another earthquake occurred in 1958. The preexisting crack pattern was considerably accentuated, especially in the transept dome that was completely demolished and rebuilt in r.c. The completion of the necessary restoration work was carried out in the seventies. The Baroque style decorations, which had concealed the original medieval one, was eliminated. During the removal works, some original structures were brought to light while others were completely reconfigured. The cross section of the two main pillars at the end of the naves were modified (Fig. 4a). The two last octagonal columns were completely rebuilt (Fig. 4b) while the others were reshaped by removing the XVIII century cruciform cover and revealing the original stone masonry. The previously lowered internal longitudinal walls, running over the central nave columns, were raised again realizing two r.c. curbs inside the wall thickness, one at the base of the new masonry and the other under the wooden trusses support (Fig. 4c).

2.3. The latest intervention until the 2009 earthquake

After the 1997 Umbria and Marche earthquake, the Basilica was subjected to some interventions to improve its seismic behavior.

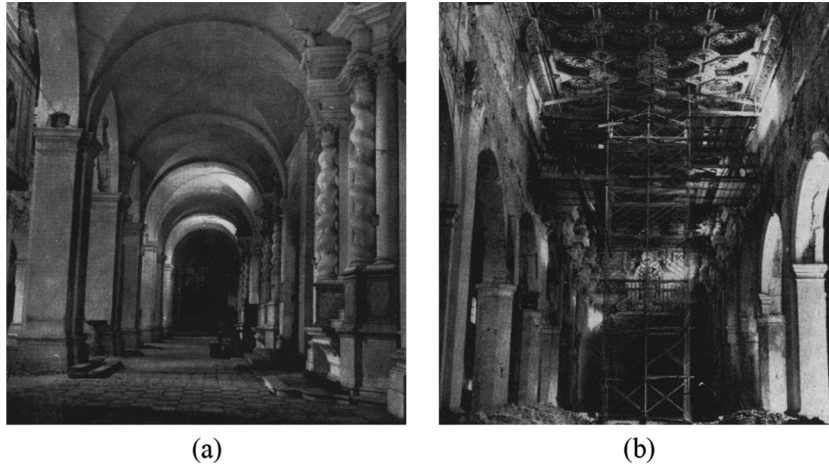


Fig. 2. (a) Aisle vaults in Baroque style, and (b) wooden ceiling in the central nave.

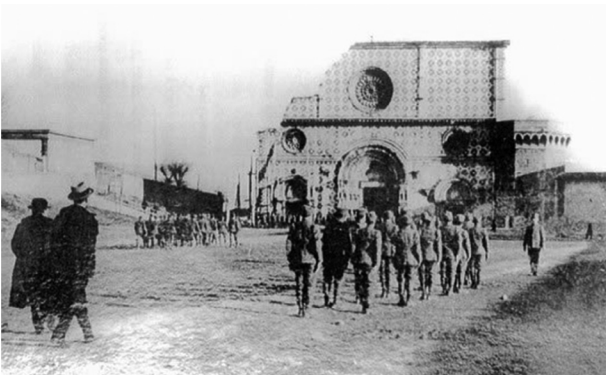


Fig. 3. Damage on the façade during the Fucino 1915 earthquake.

Strengthening of longitudinal walls was performed. A horizontal energy dissipation bracing system involving steel hysteretic dampers was installed nearly under the roof level [10,11]. The connection of the buttresses to the façade and to the longitudinal walls was improved. Drillings reinforced with steel bars and grout injections were made in the masonry walls. The façade restoration

works were in progress when the 2009 earthquake struck the city of L'Aquila.

3. Damages of 2009 L'Aquila earthquake

The earthquake occurred in L'Aquila on April 6th, 2009 was a catastrophic event for the city. The Basilica of Collemaggio was one of the most damaged historical buildings.

The earthquake caused the failure of the transept area (Fig. 5a): the dome, the barrel vaults, the triumphal arch with the above supported wall, the two main pillars and the roof structures collapsed. The analysis and the observation of the implosion mechanism suggests that the collapse was probably associated to the structural failure of the two main pillars, reshaped in seventies, supporting the transept structural system [12]. In spite of their size and apparent resistance, they proved to be vulnerable elements, owing to their weak filling material (Fig. 5b).

Large cracks were visible in the two lines of octagonal columns (Fig. 5c), developing progressively. Deep cracks initially appeared only in the central columns of the nave; then, with the aftershocks, they emerged also in almost all the others. The cracks occurred mostly in the mortar joints, but, in some cases, they involved also the stone blocks, despite their high resistance.

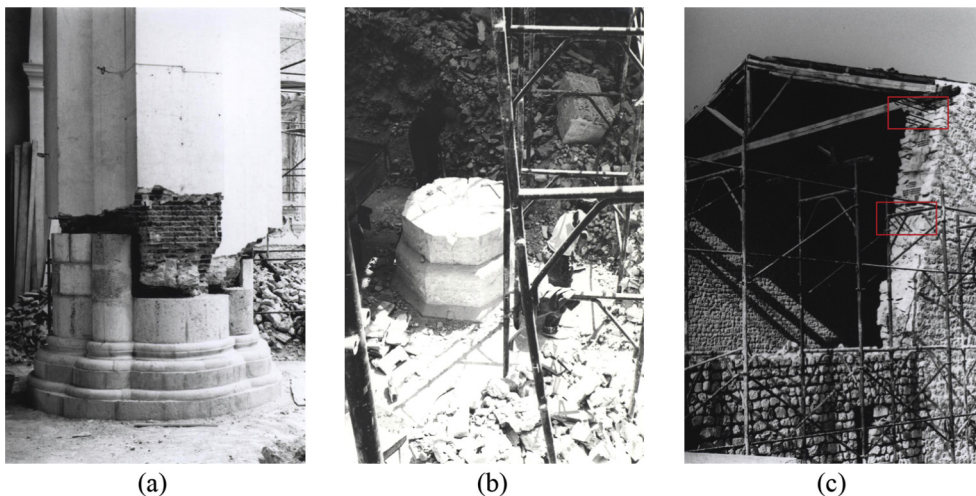


Fig. 4. (a) Reconfiguration of the main pillars with a polylobate section, (b) demolition and reconstruction of the two last octagonal columns, and (c) realization of the two r.c. curbs.

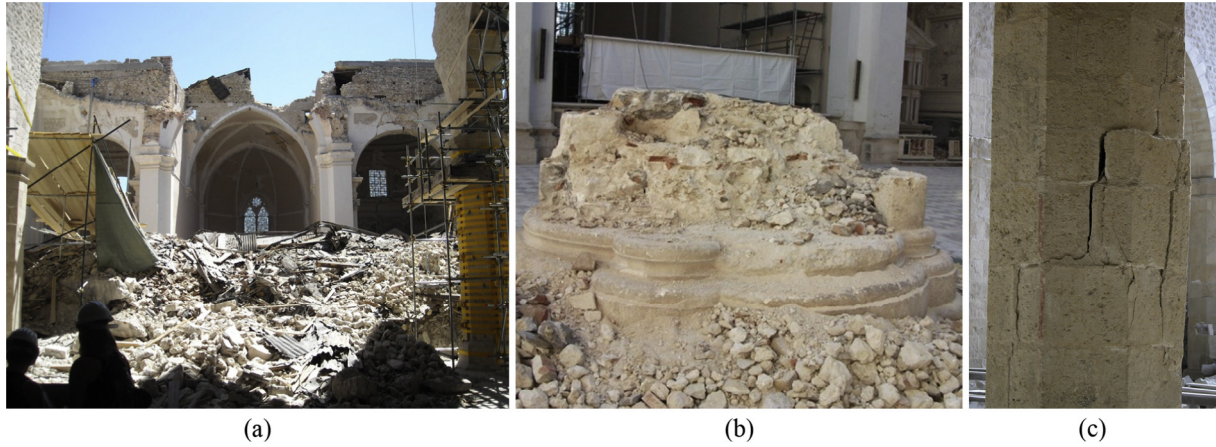


Fig. 5. (a) Collapse of the transept area, (b) one of the two main pillars with weak filling material in the core, and (c) cracks on one stone column.

The apse area also suffered serious damages: cracks appeared in the mortar joints of the outer squared stone wall and inside the apsidal vault, with partial detachment and relative displacements in one of the ribs.

4. Eigenvalue and response spectrum analyses

In order to better understand the global dynamic behavior of the Basilica of Collemaggio during the last earthquake and the effect of the seismic action on the nave columns, eigenvalue and response spectrum analyses have been performed. The 3D finite element (FE) model has been developed with Midas Gen [16] software. The geometry of the church has been reconstructed thanks to both complete laser scanner and photogrammetric survey conducted by Barazzetti et al. and Oreni et al. [17,18].

4.1. Numerical modelling

To implement the global FE model (Fig. 6), the geometry of the church has been discretized using: (i) beam element to represent columns, pillars, arches, curbs, roof trusses; (ii) plate element to represent walls and vaults. The model mesh has been adapted in order to respect as possible the geometric characteristics of the church, such as the openings and the imperfect parallelism between nave walls. The domes and the roof structures of the apse have not been modeled: their presence has been taken into account by distributing their masses on the top line of the walls.

Particular attention has been given to the non-homogeneous distribution of the physical and mechanical masonry characteristics. Different elastic moduli and mass densities were identified by the post-earthquake experimental campaign. Therefore, the modeled walls have been subdivided by regions where the mate-

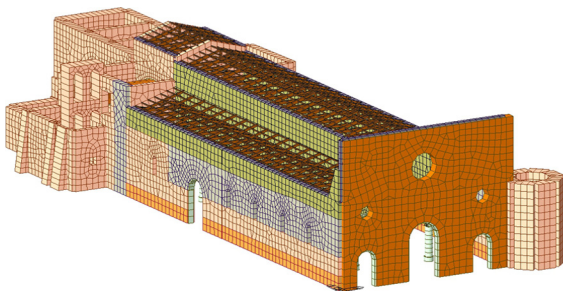


Fig. 6. General view of the FE model of the Basilica.

rial is assumed to have linear elastic behavior and homogeneous and isotropic characteristics. The mechanical properties of structural elements are listed in Table 1. When appropriate, as suggested by Italian Building Code [19], the bending and shear stiffnesses have been properly reduced to take into account the cracking in masonry brittle materials.

The self-weight and dead loads, together with their masses, have been applied to the FE model of the church. The seismic action has been introduced through the elastic response spectrum provided by Italian Building Code [19,20] as reported in Fig. 7. For the identification of the spectrum, the following parameters have been used: soil type B, topography category T1, value of nominal design life $V_n = 50$. The obtained peak ground acceleration is $a_g = 0.261$ g.

4.2. Analysis results

The results of the eigenvalue analysis showed that the building is characterized by a complex dynamic response with fragmentation of the total participating mass in different modes (Fig. 8).

Table 1
Mechanical properties of structural elements.

Elements	Material	E (MPa)	ν (-)	ρ (kN/m ³)
Walls	Masonry	800–2000	0.2	18
Columns	Stone	20,000	0.2	22
Main pillars	Masonry	1600	0.2	18
R.c. elements	Concrete	31,475	0.2	25
Roof trusses	Wood	10,000	0.2	5
Steel bracing system	Steel	210,000	0.3	78.5

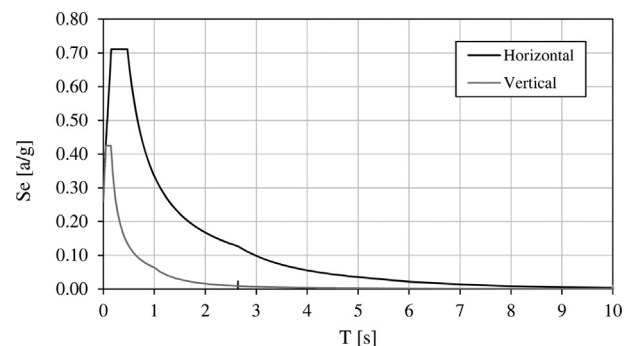


Fig. 7. Horizontal and vertical response spectrum provided by Italian Building Code.

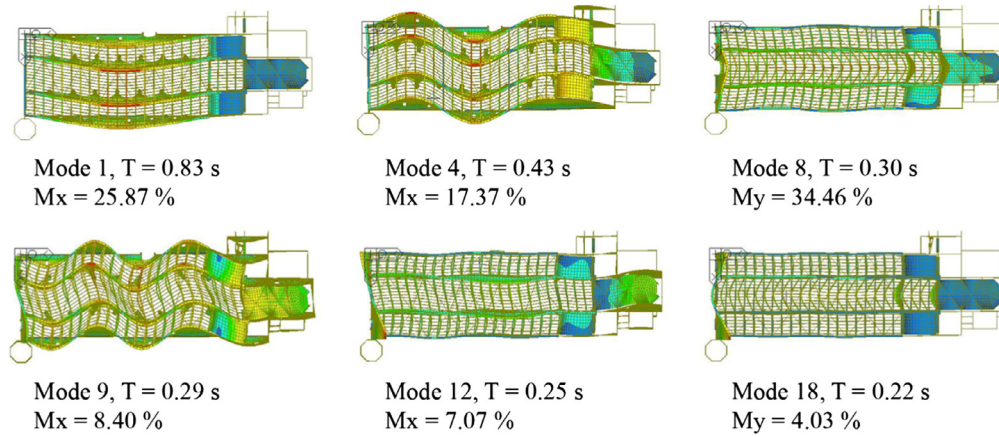


Fig. 8. Principal mode shapes of the Basilica, related periods and participating masses.

Focusing the attention on the naves behavior in transversal direction (x), the in-plane stiffness difference between the façade and the transept-frame, made by the two main pillars and the triumphal arch above them, results in an eccentricity between the center of mass G_M and the center of stiffness G_K (Fig. 9). Strong torsional effect occurs in case of transversal seismic motion, causing an increasing demand of displacement for the two main pillars. This demand, together with the low quality of the pillars masonry, is probably one of the main reasons of the transept collapse during the last earthquake, as suggested also by Gattulli et al. [12] and Arcidiacono et al. [14].

The response spectrum analysis results show important stresses on the stone-masonry columns of the nave. Table 2 reports internal forces and displacements determined for the most stressed element.

4.3. Structural verification

The structural checks of the most stressed column have been evaluated both for bending moment and for shear actions. The ver-

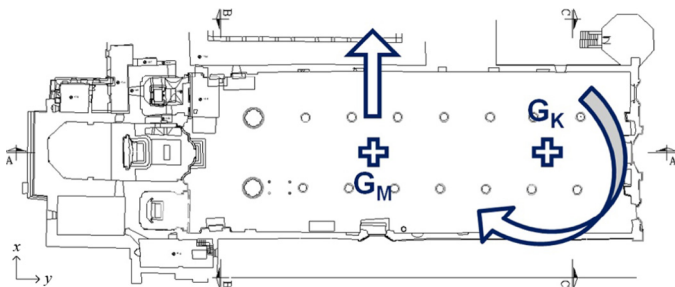


Fig. 9. Conceptual representation of the in-plan eccentricity between center of masses G_M and center of stiffness G_K .

Table 2
Demand vs. capacity for the most stressed column.

	Demand	Capacity	C/D
Moment (kN m)	4959.47	857.73 ($f_c = 16$ MPa)	0.173
		983.72 ($f_c = 24$ MPa)	0.198
		1091.84 ($f_c = 48$ MPa)	0.220
Shear (kN)	1081.98	884.28	0.817
Top displacement (cm)	2.91		

ification coefficients C/D , defined as the ratio between the capacity of the structural member and the corresponding seismic action, are listed in Table 2.

The evaluation of the flexural bearing capacity of the unreinforced masonry (URM) cross-section requires the definition of the material mechanical properties. Because of the lack of experimental stress-strain curves obtained by in-situ tests, a no-tension elastic perfectly brittle constitutive law has been adopted (Fig. 10a) in order to guarantee conservative results in comparison to elastoplastic or softening models (Parisi and Augenti [21]). Despite the simplicity of the considered constitutive law, the selection of correct values of masonry Young modulus E and compressive strength f_c is challenging in the case of non-standard masonry assemblages. Different aspects have to be taken into account in the estimation of f_c : (a) the average dimension of the blocks (300 mm) is sensibly greater than the thickness of the mortar joints (5 mm); (b) due to the degradation of the mortar during the years, the strength of the joints is extremely lower compared to the resistance of the stone blocks. Classical methods, proposed by international codes [22], evaluate the compressive resistance of masonry as a combination between the strength of the unit blocks and the strength of mortar cubes. In the case of regular assemblage of solid/hollow clay bricks, the overall compressive strength can be assumed as 0.35 times the resistance of the unit [23]. Nevertheless, studies conducted by Kaushik et al. [24] have shown that the reliability of these approaches is too conservative, especially when unit blocks exhibits high compressive strengths. Moreover, when dealing with masonry components subjected to bending, the usual Hayman's hypothesis [25] of masonry unlimited resistance in compression is considered. This assumption has been recently adopted for the specific case of URM columns [26].

In order to find a reasonable compromise between the two approaches, the value of the compressive strength f_c is assumed equal to the resistance of the stone blocks. In particular, due to the variability of the stone typology, three different levels of f_c are considered: 16 MPa, 24 MPa and 48 MPa, trying to reproduce the results of experimental compressive tests conducted on six stone cubic specimens. According to the columns sonic tests performed before the earthquake [5], Young modulus $E = 20,000$ MPa is assumed. The linear relation between stress and strain, i.e. $\varepsilon = \sigma/E$, provides three levels of ultimate strain ε_u : 0.0008, 0.0012, 0.0024.

The shear capacity F_{vk} of the column is evaluated with the formula proposed by the Italian Building Code [19] ($F_{vk} = 0.4 N_0$ where N_0 is the column axial load), neglecting the shear strength of the mortar.

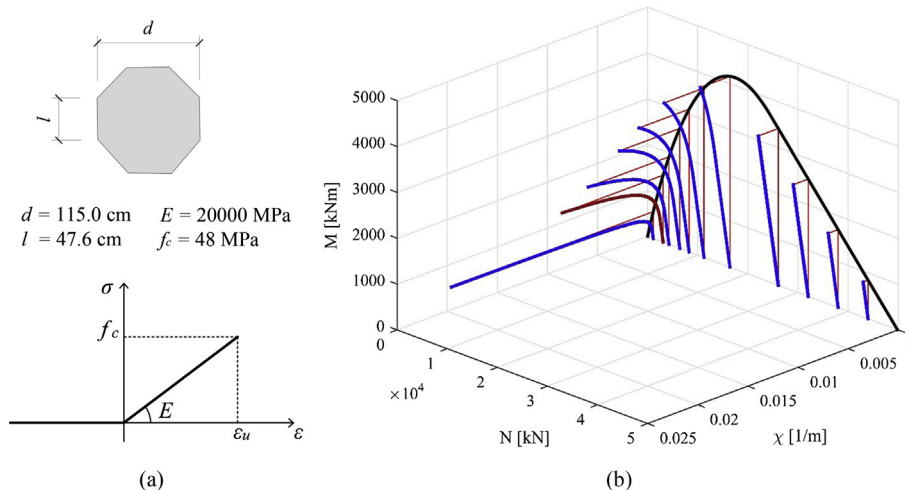


Fig. 10. (a) Geometry, constitutive law and (b) 3D $M-N-\chi$ diagram of the cross section of the column.

5. Non-linear analysis of stone masonry column

Non-linear analyses on nave columns have been conducted in order to better understand their seismic response. Even if cracks occurred, these structural elements showed a good resistance under transversal loads during the last earthquake, as compared with the results of the response spectrum analysis that estimates an high vulnerability level.

The main reason of columns structural performance could be recognized in two aspects: (i) the good compressive strength of the stone material; (ii) the low level of axial load acting on the top of the columns in comparison to their strength. The two aspects are strongly correlated each other as it can be observed in the 3D diagram (Fig. 10b) representing the $M-N$ domain of the octagonal cross section of the column and the $M-\chi$ moment-curvature curves at different levels of axial loads.

The sectional analysis showed that the ductility of the column cross-section increases by reducing the axial load applied to the column. Particularly, for axial load levels of approximately 2000 kN (red¹ curve in Fig. 10b) the column exhibits significant curvatures without losing resistance. Considering the three increasing levels of stone compressive strength f_c (16 MPa, 24 MPa and 48 MPa), it is possible to appreciate a stronger change in ductility than in bending resistance (Fig. 11).

Owing to these considerations, a non-linear analysis of a representative column has been implemented to understand its real behavior. The column geometry is reported in Fig. 12 and its geometrical characteristics are collected in Table 3.

5.1. State of the art on non-linear analyses of masonry columns

The non-linear seismic behavior of URM columns has been deeply studied in the past using both numerical and analytical methods.

Looking at the numerical techniques, the FE method is certainly the most common one adopted for the assessment of masonry buildings [27]. Particularly, the discretization of the structure can be performed following three approaches: (I) detailed micro-modelling, bricks and mortar joints are represented by continuum elements; (II) simplified micro-modelling, bricks are modeled by continuum elements while mortar joints are lumped in discontin-

uous interface elements; (III) macro-modelling, bricks and mortar are smeared out in an homogeneous continuum [4]. Applications and comparisons between the approaches for non-linear modelling of URM columns can be found in Giordano et al. [28] and in Roca et al. [29].

Remarkable numerical investigations have been also carried out thanks to the Discrete Element method (DE), first developed by Cundall in 1971 for the analysis of rock block systems [30]. According to this approach, the masonry column is subdivided in a discrete number of rigid (or elastic) bodies connected through contact joints able to represent the mutual interaction between masonry blocks. Application of this technique on stone masonry columns has been presented by Psycharis et al. [26] for the case of Parthenon Pronaos. Nevertheless, as remarked by Lemos [31], the capability of DE technique is limited to the definition of the collapse mechanism of the structure but it is not indicated for a state-of-stress evaluation inside the masonry blocks.

Regarding the analytical models, most of them start from the first studies of Frish-Fay [32] about the stability of masonry piers and are based on one-dimensional-beam theory under the assumption that axial strains behave linearly in bending, i.e. sections remain plane. While several procedures are available in literature for elements subjected to eccentric vertical loads [33,34], only few methods have been studied in the case of horizontal forces. In 1995, La Mendola et al. [35] proposed an analytical model for the evaluation of the out-of-plane capacity curve of a masonry wall, assuming a no tensile resistance material and unlimited strength in compression. This model has been further developed by Gurel and Pekgokgoz [36], who extended the algorithm to the case of circular cross-sections, including the effect of vertical imperfections and eccentricity of the applied static load. These analytical procedures, compared to the numerical ones, follow in a quick determination of the results with a consequent reduction of computational costs, by means of a simple scripting process.

In the following, a comparison between the results obtained with an analytical and a numerical (FE) approach is reported.

5.2. Analytical model

Firstly, a non-linear analytical model of the column, based on the formulation proposed by La Mendola [35] and Gurel and Pekgokgoz [36], has been implemented.

The octagonal masonry column is represented by an equivalent cantilever divided in two cylindrical portions. The height of these portions are respectively equal to $h_b = 0.81 \text{ m}$ (Lower + Upper base)

¹ For interpretation of color in Fig. 10, the reader is referred to the web version of this article.

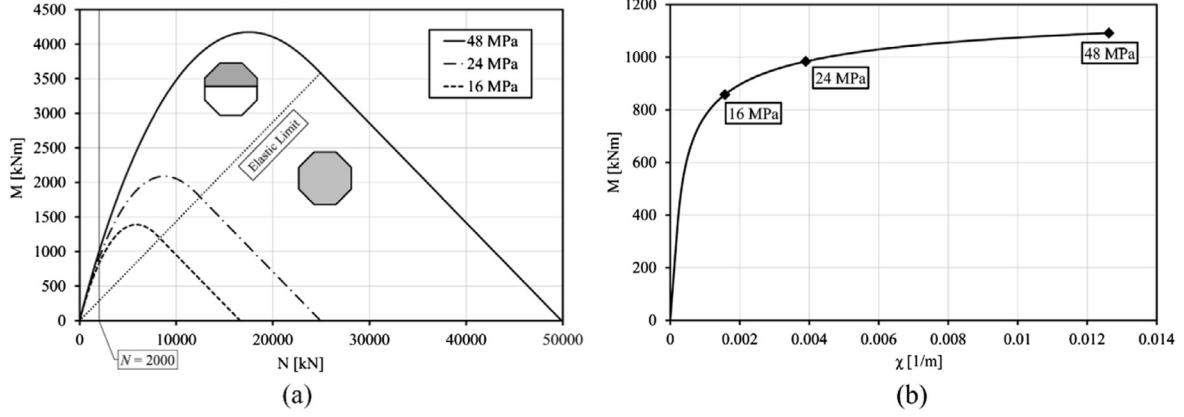


Fig. 11. M - N (a) and M - χ (b) diagrams for different levels of f_c .

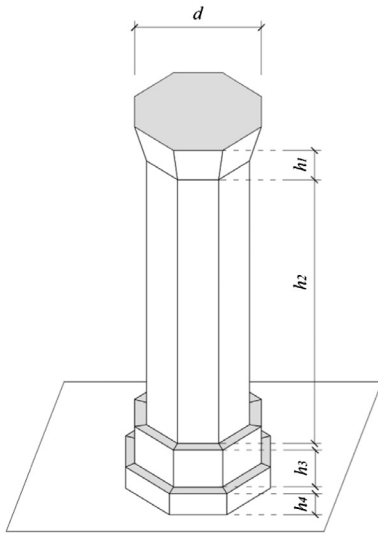


Fig. 12. Geometry of the column.

Table 3
Geometrical characteristics of the column.

Geometry	Section d (m)	Height h (m)
h_1 Capital	1.27	0.54
h_2 Column	1.15	3.60
h_3 Upper base	1.40	0.51
h_4 Lower base	1.60	0.30
Total	-	4.95

and $h_f = 4.14$ m (Column + Capital). The two diameters are evaluated by assuming an equivalent volume rule with respect to the real structure.

The column is discretized into $n = 13$ finite elements, equal to the number of its block layers: the first 12 elements have the same height $h_e = h_f/(n - 1)$; the last element has $h_e = h_b = 0.81$ m. These elements are numbered from 1 to n , starting from the top, and bounded by $n + 1$ sections, numbered from 0 to n (Fig. 13).

The column is subjected to its self-weight W and to a vertical force N representing the applied loads on the top. Due to the symmetric position of the arches above the column, the eccentricity of the vertical force is considered equal to zero. The seismic load is defined by an inverted triangular static lateral load distribution f

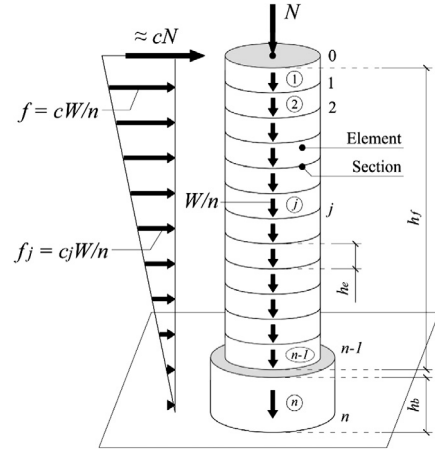


Fig. 13. Discretized model and loading condition.

that tries to take into account the fundamental vibration mode shape of the structure. Moreover, a concentrated lateral seismic force F is applied at the top of the column, representing the effect of the sustained masses. The loads f and F are defined by the Eqs. (1) and (2), where c is the seismic coefficient describing the intensity of earthquake loading.

$$f_j = c_j \cdot \frac{W}{n} = c \cdot \frac{(n - j + 1/2)}{(n - 1/2)} \cdot \frac{W}{n} \quad (1)$$

$$F = c \cdot N \quad (2)$$

The deformed shape of the column is assumed as a combination of successive cylindrical segments. The method assumes a constant curvature inside each element, equal to its value on the upper section. Considering a system of coordinates $O(z, v)$ having the z axis aligned with the vertical top load N , the dimensionless eccentricity e_j of the j -th cross section can be defined as:

$$e_j = \frac{v_j}{d} - \frac{1}{(n \frac{N}{W} + j)} \sum_{i=1}^j \frac{v_{Gi}}{d} + c \cdot \xi \cdot j \cdot n \cdot \frac{N/W}{(n \frac{N}{W} + j)} + c \cdot \xi \cdot \frac{1}{(n - 1/2) \cdot (n \frac{N}{W} + j)} \cdot \sum_{i=1}^j (n - i + 1/2)(j - i + 1/2) \quad (3)$$

where v_j and v_{Gi} are respectively the centroid coordinate of the j -th cross section and the centroid coordinate of the i -th element (depending on the rotation of the top cross-section β); φ_{ij} is the cur-

vature of the generic element or cross-section and $\xi = h_e/d = h/nd$ is the discretization parameter.

Assuming a no-tension material, the curvature of an element depends on whether its upper cross-section is uncracked or partially cracked. Therefore, following this hypothesis, if the axial load is within the section kern, the section will remain uncracked, otherwise it will be partially cracked. It is well known that the kern of a circular section with diameter d is a circle with the same center, having a radius of $d/8$. When $e_j/d \leq 1/8$, the linear elastic formulation can be assumed for the moment curvature relation:

$$\phi_{j+1} = \frac{N_j \cdot e_j}{EI} \quad (4)$$

where E is the masonry modulus of elasticity and I is the moment of inertia of the cross-section about its centroid axis.

Otherwise, when the cross-section is partially cracked, the curvature cannot be easily expressed because the position of neutral axis a cannot be calculated in closed form. In general, a trial-and-error procedure is needed to determine the neutral axis depth and then calculate $\sigma_{\max} = \sigma_0$, $\varepsilon_{\max} = \varepsilon_0$ and the curvature, as suggested by Gurel and Pekgokgoz [36] according to the following Eqs. (5) and (6):

$$a \cong \frac{1}{2} \left[2.33 \cdot \left(1 - 2 \frac{e_j}{d} \right) + 0.58 \cdot \left(1 - 2 \frac{e_j}{d} \right)^3 \right] \cdot d \quad (5)$$

$$\sigma_0 \cong 4 \cdot \left[\frac{0.372 + 0.056 \cdot \left(1 - 2 \frac{e_j}{d} \right)}{\left(1 - 2 \frac{e_j}{d} \right)^{3/2}} \right] \frac{N_j}{d^2} \quad (6)$$

Then, the curvature in the partially cracked cross-section can be written as (7):

$$\phi_{j+1} = \frac{\varepsilon_0}{a} = \frac{\sigma_0}{Ea} \quad (7)$$

More details concerning the analytical formulation could be found in [35,36].

This analytical procedure is able to calculate the capacity curve of the column until the collapse for equilibrium loss. Obviously, depending on the geometry of the column and the vertical applied load N , it is possible to reach the ultimate compressive strength or the maximum frictional shear resistance in one section, before the collapse for equilibrium loss.

5.3. Finite element model

In order to validate the reliability of the previous analytical model, a non-linear FE model of the column has been developed (Fig. 14) with the software Midas FEA [37]. Since the stone blocks itself exhibit a good resistance in compression, linear elastic solid elements have been used for their discretization. The considered mechanical characteristics are listed in Table 1. According to the approach proposed by Lourenco in 2002 [4], a simplified micro-modelling has been adopted: mortar joints are discretized using non-linear lumped interfaces elements, with a Mohr-Coulomb constitutive law. The normal and tangent elastic fictitious stiffnesses are assumed as $k_N = k_T = 1.000 \cdot E \cdot d$ (d = characteristic dimension of the finite element), cohesion equal to zero, internal friction angle $\varphi = 21.80^\circ$, dilatancy angle equal to zero. Analyses have been conducted using both first and second order hypothesis for the displacements. Regarding the applied loads, two sequential load stages have been considered: in the first a vertical load N (as a constant distribution of pressures on the capital) and self-weight have been applied; in the second one horizontal seismic forces, coherent with the analytical model, have been imposed. In both stages, Newton-Raphson integration method has been used for the solution of the non-linear problem.

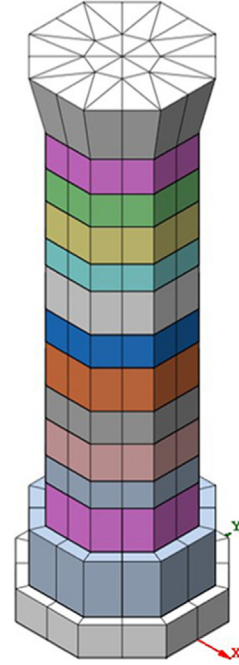


Fig. 14. Finite element model of the column.

6. Discussion of the results

The capacity curves of the column are reported in Fig. 15. The results are expressed in terms of top displacement and base shear of the column. The solid line is related to the analytical model: it could be appreciated that the material failure in compression occurs before the equilibrium loss of the column. In particular, according to the moment curvature diagrams of the section, the increase of f_c causes an increase of the element ductility from 9.8 mm, for 16 MPa, to 34.7 mm, for 48 MPa. Moreover, the results highlight that failure for the overcome of frictional shear resistance (884.28 kN) is never reached.

A good matching in the results can be found looking at the finite element analyses capacity curves: the dashed line, evaluated with the hypothesis of first order displacements, reaches the value of stone strength for displacements close to the analytical ones. Passing from the first order to the second order hypothesis, the comparison is even better. Residual differences between analytical and FE model could be further reduced by refining the mesh of the horizontal interfaces. Also in the FE analyses, failure for shear sliding is not detected. The progressive reduction of the column compressed zone is shown in Fig. 16a: the activation of the horizontal interfaces causes a decrease of secant stiffness and a conse-

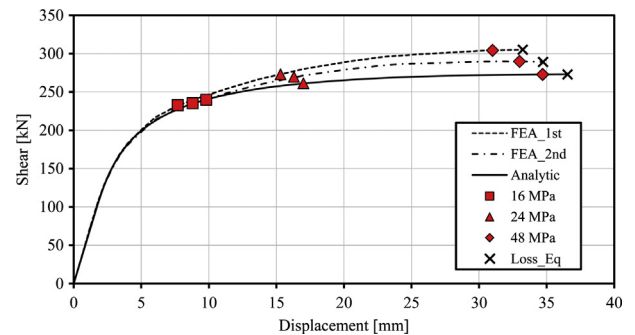


Fig. 15. Capacity curves for analytical approach and FE analyses (with first and second order hypothesis for the displacements).

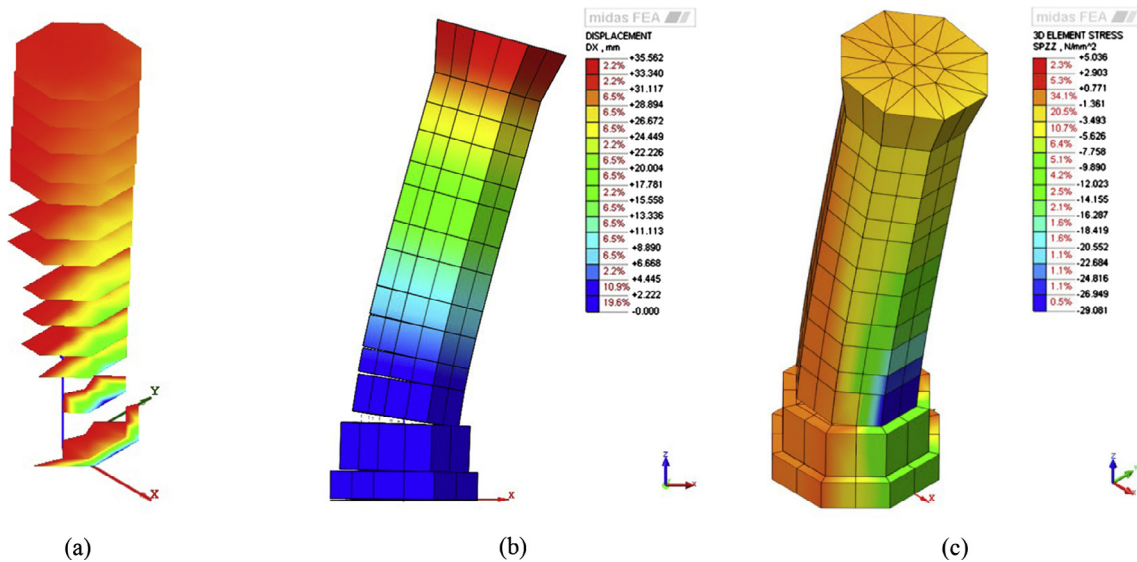


Fig. 16. Analysis results: (a) activation of non-linear interfaces, (b) amplified deformed shape, and (c) concentration of vertical stresses at the base of the column.



Fig. 17. Earthquake damage at the base of the column.

quent increase of horizontal displacement (Fig. 16b). The concentration of vertical stresses at the base of the column, evident from the post-earthquake inspection (Fig. 17), is also caught by the model (Fig. 16c).

7. Conclusions

Seismic assessment of the Basilica of Collemaggio in L'Aquila is presented, focusing the attention on the behavior of the stone masonry columns of the naves. A first overall finite element model of the church, made by shell and beam elements, has been implemented considering the information obtained from the recent accurate survey together with the mechanical parameters determined from some in-situ tests. Eigenvalue and response spectrum analyses have been performed: the results showed a complex structural dynamic behavior and, in particular, a significant seismic demand on the nave columns resulting in a vulnerability level C/D less than one. This result seems to be in contrast with the real response of the elements during 2009 L'Aquila earthquake.

To better understand the real behavior of the columns, non-linear analyses have been implemented using both analytical and numerical approaches. Thanks to the good compressive strength of the stone blocks (between 16 MPa and 48 MPa), the redistribution of the stresses in the structural element allows a ductile

behavior of the column that increases with the increase of the material quality. Particularly, the horizontal drift of the column, coming from the global finite element model, has resulted less than the maximum displacement capacity evaluated by the non-linear analyses. These results could justify the capacity of the columns to withstand last earthquake without collapsing.

Acknowledgments

The authors acknowledge the research group of Prof. Dante Galeota, from L'Aquila University, for the scientific and technical collaboration in the restoration project of the Basilica S. Maria di Collemaggio, financially supported by ENI Spa. Thanks also to G. Riva and F. Tassoni for the contribution given during the development of their master thesis.

References

- [1] Penna A. Seismic assessment of existing and strengthened stone-masonry buildings: critical issues and possible strategies. *Bull Earthquake Eng* 2015;13:1051–71.
- [2] Ronca P. The significance of the gauging system in the flatjack in-situ test. *TMS J* 1996;14(1).
- [3] Franchi A, Crespi P, Ronca P, Pizzamiglio F. An in situ diagonal compression test for brick walls with displacement control on the two external layers. *Int J Hous Sci Appl* 2014;38:25–35.
- [4] Lourenco PB. Computations on historic masonry structures. *Prog Struct Mat Eng* 2002;4:301–19.
- [5] Antonacci E, Beolchini GC, Di Fabio F, Gattulli V. Retrofitting effects on the dynamic behaviour of S. Maria di Collemaggio. *Comput Eng* 2001:479–88.
- [6] Ranalli D, Scozzafava M, Tallini M. Ground penetrating radar investigations for the restoration of historic buildings: the case study of the Collemaggio Basilica (L'Aquila, Italy). *J Cult Heritage* 2004;5:91–9.
- [7] Cimellaro GP, Reinhorn AM, De Stefano A. Introspection on improper seismic retrofit of Basilica Santa Maria di Collemaggio after 2009 Italian earthquake. *Earthq Eng Eng Vib* 2011;10:153–61.
- [8] Cimellaro GP, Reinhorn AM, De Stefano A. Reply to "discussion 1 on 'introspection on improper seismic retrofit of Basilica Santa Maria di Collemaggio after 2009 Italian earthquake' by G.P. Cimellaro, A.M. Reinhorn and A. De Stefano" by Vincenzo Ciampi. *J Earthq Eng Eng Vib* 2012;11:283–8.
- [9] Cimellaro GP, Reinhorn AM, De Stefano A. Reply to "discussion 2 on 'introspection on improper seismic retrofit of Basilica Santa Maria di Collemaggio after 2009 Italian earthquake' by G.P. Cimellaro, A.M. Reinhorn and A. De Stefano" by Enzo Cartapati. *J Earthq Eng Eng Vib* 2012;11:291–2.
- [10] Cartapati E. Discussion 2 on "introspection on improper seismic retrofit of Basilica Santa Maria di Collemaggio after 2009 Italian earthquake" by G.P. Cimellaro, A.M. Reinhorn and A. De Stefano. *J Earthq Eng Eng Vib* 2012;11:289–90.
- [11] Ciampi V. Discussion 1 on "introspection on improper seismic retrofit of Basilica Santa Maria di Collemaggio after 2009 Italian earthquake" by G.P.

- Cimellaro, A.M. Reinhorn and A. De Stefano. *J Earthq Eng Eng Vib* 2012;11:281–2.
- [12] Gattulli V, Antonacci E, Vestroni F. Field observations and failure analysis of the Basilica S. Maria di Collemaggio after the 2009 L'Aquila earthquake. *Eng Fail Anal* 2013;34:715–34.
- [13] Potenza F, Federici F, Lepidi M, Gattulli V, Graziosi F, Colarieti A. Long-term structural monitoring of the damaged Basilica S. Maria di Collemaggio through a low-cost wireless sensor network. *J Civ Struct Health Monit* 2015;5:655–76.
- [14] Arcidiacono V, Cimellaro GP, Ochsendorf JA. Analysis of the failure mechanisms of the basilica of Santa Maria di Collemaggio during 2009 L'Aquila earthquake. *Eng Struct* 2015;99:502–16.
- [15] Bartolomucci C. Santa Maria di Collemaggio. Interpretazione critica e problemi di conservazione. Roma: Palombi Editori; 2004.
- [16] Midas Gen. Analysis manual 2015.
- [17] Barazzetti L, Brumana R, Oreni D, Previtali M, Ronconi F. UAV-based orthophoto generation in urban area: the Basilica of Santa Maria di Collemaggio in L'Aquila. In: Computational science and its applications – ICCSA 2014, proceedings, part IV. p. 1–13.
- [18] Oreni D, Brumana R, Banfi F, Bertola L, Barazzetti L, Cuca B, Previtali M, Roncoroni F. Beyond crude 3D models: from point clouds to historical building information modeling via NURBS. Digital heritage. Progress in cultural heritage: documentation, preservation, and protection 2014:166–75.
- [19] NTC. Nuove norme tecniche per le costruzioni. Roma: Ministero delle Infrastrutture e dei Trasporti; 2008.
- [20] Circolare n. 617 del 2 febbraio. Istruzioni per l'Applicazione Nuove Norme Tecniche Costruzioni di cui al Decreto Ministeriale 14 gennaio 2008. Roma: Ministero delle Infrastrutture e dei Trasporti; 2009.
- [21] Parisi F, Augenti N. Assessment of unreinforced masonry cross sections under eccentric compression accounting for strain softening. *Constr Build Mater* 2013;41:654–64.
- [22] EN 1996-1-1:2005. Eurocode 6: design of masonry structures – Part 1–1: general rules for reinforced and unreinforced masonry structures. Brussels: Comité Européen de Normalisation; 2005.
- [23] Bennett RM, Boyd KA, Flanagan RD. Compressive properties of structural clay tile prisms. *J Struct Eng ASCE* 1997;123(7):920–6.
- [24] Kaushik H, Rai D, Jain S. Stress–strain characteristics of clay brick masonry under uniaxial compression. *J Mater Civ Eng ASCE* 2007;19:728–39.
- [25] Heyman J. The stone skeleton. *Int J Solides Struct* 1966;2:269–79.
- [26] Psycharis IN, Lemos JV, Papastamatiou DY, Zambas C, Papantonopoulos C. Numerical study of the seismic behaviour of a part of the Parthenon Pronaos. *Earthq Eng Struct Dynam* 2003;32:2063–84.
- [27] Roca P, Cervera M, Gariup G, Pelà L. Structural analysis of masonry historical constructions, classical and advanced approaches. *Arch Comput Methods Eng* 2010;17:299–325.
- [28] Giordano A, Mele E, De Luca A. Modelling of historical masonry structures: comparison of different approaches through a case study. *Eng Struct* 2002;24:1057–69.
- [29] Roca P, Cervera M, Pelà L, Clemente R, Chiumenti M. Continuum FE models for the analysis of Mallorca Cathedral. *Eng Struct* 2013;46:653–70.
- [30] Cundall PA. A computer model for simulating progressive large scale movements in blocky rock systems. In: Proceedings of the symposium on rock fracture (ISRM), vol. 1, paper II-8. Nancy, France.
- [31] Lemos JV. Discrete element modeling of masonry structures. *Int J Archit Heritage* 2007;1:190–213.
- [32] Frisch-Fay R. Stability of masonry piers. *Int J Solids Struct* 1975;11(2):187–98.
- [33] De Falco A, Lucchesi M. No tension beam-columns with bounded compressive strength and deformability undergoing eccentric vertical loads. *Int J Mech Sci* 2007;49:54–74.
- [34] Fossetti M, Giacchino C, Minafò G. Stability analysis of clay brick masonry columns: numerical aspects and modelling strategies. *Mater Struct* 2015;48:1615–25.
- [35] La Mendola L, Papia M, Zingone G. Stability of masonry walls subjected to seismic transverse forces. *J Struct Eng – ASCE* 1995;121(11):1581–7.
- [36] Gurel MA, Pekgokgoz RK. Strength capacity of unreinforced masonry cylindrical columns under seismic transverse forces. *Bull Earthq Eng* 2012;10:587–613.
- [37] Midas FEA. Analysis manual 2015.